Development 134, 1431-1441 (2007) doi:10.1242/dev.02828

Shroom family proteins regulate γ-tubulin distribution and microtubule architecture during epithelial cell shape change

Chanjae Lee, Heather M. Scherr and John B. Wallingford*

Cell shape changes require the coordination of actin and microtubule cytoskeletons. The molecular mechanisms by which such coordination is achieved remain obscure, particularly in the context of epithelial cells within developing vertebrate embryos. We have identified a novel role for the actin-binding protein Shroom3 as a regulator of the microtubule cytoskeleton during epithelial morphogenesis. We show that Shroom3 is sufficient and also necessary to induce a redistribution of the microtubule regulator γ-tubulin. Moreover, this change in γ-tubulin distribution underlies the assembly of aligned arrays of microtubules that drive apicobasal cell elongation. Finally, experiments with the related protein, Shroom1, demonstrate that γ-tubulin regulation is a conserved feature of this protein family. Together, the data demonstrate that Shroom family proteins govern epithelial cell behaviors by coordinating the assembly of both microtubule and actin cytoskeletons.

KEY WORDS: Shroom, gamma-tubulin, microtubule, neural tube defect, morphogenesis, *Xenopus*

INTRODUCTION

Cell shape change is a central mechanism for morphogenesis in multicellular organisms. One ubiquitous cell shape change is apical constriction, by which polarized epithelial cells reduce their apical surface area while the basal surface remains unchanged or expands (Fristrom, 1988). This process converts columnar cells into wedge-shaped cells, facilitating the bending of cell sheets. One peculiarity of apical constriction is that this cell shape change is almost uniformly linked to another cell shape change, apicobasal cell elongation. An increase in cell length is observed in apically constricting cells in organisms ranging from *Volvox* to arthropods and vertebrates (e.g. Schroeder, 1970; Sweeton et al., 1991; Viamontes and Kirk, 1977).

Whereas the molecular control of apical constriction has been at least partially defined (see below), the molecules governing apicobasal cell elongation remain almost entirely obscure. Electron microscopy and inhibitor studies have implicated microtubules (MTs) as the causative cytoskeletal agent in cell elongation, but how discrete populations of MTs are assembled as embryonic epithelial cells change shape remains unclear (Brun and Garson, 1983; Burnside, 1973; Karfunkel, 1971; Messier, 1978; Schroeder, 1970). In other epithelial cell types, apicobasally aligned MTs are assembled from a diffuse microtubule-organizing center (MTOC) beneath the apical surface (Bacallao et al., 1989; Bre et al., 1990; Meads and Schroer, 1995; Rizzolo and Joshi, 1993). One central regulator of MT assembly is γ-tubulin, a minus-end anchoring protein that is a component of the protein complex that nucleates MTs (Gunawardane et al., 2000; Job et al., 2003; Stearns et al., 1991). γ-tubulin is probably a key player in the assembly of the robust MT arrays observed in elongating neural epithelial cells, but how its activity may be regulated during cell shape change in developing embryos has not been addressed.

Apicobasal cell elongation is tightly linked to apical constriction. Because the MT and actin cytoskeletons are often jointly regulated (Rodriguez et al., 2003), we asked whether molecules governing apical constriction were also required for cell elongation. Recently, we found that the novel protein Shroom3 was sufficient to drive apical constriction and apical actin accumulation in naïve cells, suggesting that this protein lies near the top of the molecular hierarchy controlling this cell behavior (Haigo et al., 2003). Moreover, this actin-binding protein is essential for neural tube closure in both mice and frogs (Haigo et al., 2003; Hildebrand and Soriano, 1999). Shroom3 (previously simply known as Shroom) is a member of a new family of proteins, all of which have been associated with the actin cytoskeleton (Hagens et al., 2006). These proteins were renamed recently to reflect the similarities of the proteins within the family and to reflect the order in which they were identified (Hagens et al., 2006).

In this study, we show that Shroom family proteins govern MT architecture in developing epithelia. We show that Shroom3 is both necessary and sufficient to induce a redistribution of the MT regulator γ-tubulin, and that this action underlies the assembly of robust, parallel MTs that drive apicobasal cell elongation. Shroom3 is thereby necessary and sufficient to drive both apicobasal cell elongation and apical constriction in the neural epithelium during neural tube closure. Experiments with the related protein, Shroom1, demonstrate that the control of γ-tubulin distribution is a conserved feature of this protein family. In light of our previous finding that Shroom3 is sufficient to drive actin-based apical constriction (Haigo et al., 2003), the data presented here demonstrate that Shroom family proteins govern distinct epithelial cell behaviors by coordinating assembly of actin and tubulin cytoskeletons. These results thus identify a novel mechanism by which actin and MT cytoskeletons are coordinated to control cell shape in developing embryos.

MATERIALS AND METHODS

Cloning of *Xenopus* Shroom3

To facilitate studies of Shroom3 function in *Xenopus*, we have cloned full-length *Xenopus Shroom3* (see Fig. S4A in the supplementary material). Using primers based on the genomic sequence of *Xenopus tropicalis* and from available expressed sequence tags (ESTs), we obtained a partial cDNA

Department of Molecular Cell and Developmental Biology, and Institute for Cellular and Molecular Biology, University of Texas, Austin, TX 78712, USA.

*Author for correspondence (e-mail: wallingford@mail.utexas.edu)

Accepted 19 January 2007

sequence of Shroom3. To clone full-length *Xenopus Shroom3*, primers were designed from this partial sequence and 5′ RACE was performed using FirstChoice RLM-RACE Kit (Ambion). Gene-specific primers for 5′ RACE were 5′-ACTCTTCTGAGATTCCACGCTGT-3′ and 5′-TCACTGC-GAGTAGGAGGCATA-3′. Based on a full-length Xenopus Shroom3 sequence from RACE, four primer sets were designed, and a full-length cDNA was obtained by PCR and was cloned into CS107, a standard *Xenopus* vector used for transcription of capped mRNA.

Shroom3 encodes a protein with high similarity to mouse Shroom3S isoform (36% identical, 48% similar). No evidence was found for a PDZ-containing Shroom3L form in *Xenopus*. Like Shroom3S, Shroom3 lacks a PDZ at the N-terminus. Three lines of evidence suggest that the PDZ-containing Shroom3L splice form does not exist in *Xenopus*. First, repeated attempts using 5′ RACE failed to identify a PDZ-containing Shroom3 splice form. Second, no PDZ-containing sequence could be found in the *tropicalis* genome within >100 kb upstream of Shroom3. Third, BLAST searches of available *Xenopus* ESTs failed to identify a PDZ-containing XShroom3 cDNA. Like the mouse orthologs, Shroom3 expression was sufficient to induce apical actin accumulation and apical constriction (see Fig. S4B-E in the supplementary material) (see also Haigo et al., 2003).

Morpholino, DNA and mRNA injection

Capped mRNA was synthesized using mMessage mMachine kit (Ambion). DNA, mRNA or antisense morpholino oligonucleotide (Haigo et al., 2003) was injected into one or two dorsal blastomeres at the four-cell stage. Embryos were incubated until appropriate stages and were fixed in MEMFA (Davidson and Wallingford, 2005). Embryos were staged according to Nieuwkoop and Faber (Nieuwkoop and Faber, 1994).

Actin filament staining

Two units of Alexa Fluor-green-phalloidin (Molecular Probes) in methanol were completely dried before use and were resuspended in 500 μl of PBT (PBS plus 0.1% Tween 20). Fixed embryos were rinsed with PBT and were stained with the phalloidin solution at 4°C overnight. To visualize nuclei, DAPI (4 μg/ml, Sigma) or propidium iodide (20 μg/ml, Sigma) was added to phalloidin solution.

Immunohistochemistry and in situ hybridization

Fixed embryos were dehydrated completely in methanol and were bleached in 10% hydrogen peroxide and 67% methanol for 3 hours and rehydrated consecutively with TBS (155 mM NaCl, 10 mM Tris-Cl, pH 7.4). To reduce autofluorescence of yolk platelets, the embryos were incubated with 100 mM $NaBH_4$ in TBS for 4 hours at room temperature or overnight at 4°C and rinsed in TBST (0.1% Triton X-100 in TBS).

Primary antibodies used were monoclonal anti-α-tubulin antibody (1:400 dilution, DM1A; Sigma), rabbit polyclonal anti-γ-tubulin antibodies [1:200 dilution (Abcam) or as in Stearns et al. (Stearns et al., 1991); identical results were obtained with either of the two different γ-tubulin antibodies (data not shown)], polyclonal rabbit ZO-1 antibody (1:200 dilution; Zymed Laboratories) and monoclonal anti-Myc antibody (1:300 dilution, clone9E10; Abcam).

Antibodies were diluted in fetal bovine serum (FBS) solution [TBS containing 10% FBS and 5% dimethyl sulfoxide (DMSO)]. Primary antibodies were detected with Alexa Fluor-488 goat anti-mouse immunoglobulin G (IgG) (Molecular Probes), Alexa Fluor-488 goat anti-rabbit IgG (Molecular Probes) or Alexa Fluor-555 IgG (Molecular Probes) diluted 1:250 in FBS solution. To stain nuclei, propidium iodide or DAPI was added in secondary antibody solution. Embryos were cleared in Murray's Clear solution (benzyl benzoate:benzyl alcoho1, 2:1).

In situ hybridization was performed according to Sive et al. (Sive et al., 2000), with digoxygenin-labeled, antisense full-length probes to *Xenopus* Shroom3 and Shroom1 (previously known as APX) (Staub et al., 1992).

Imaging and image analysis

Imaging procedures were generally as described in Davidson and Wallingford (Davidson and Wallingford, 2005). Phalloidin-stained intact embryos in PBT were placed on a culture dish and embryos cleared in Murray's solution were placed in a culture chamber with a cover-glass bottom. For cross-sections, embryos were embedded in 2% agarose, and thick (250-300 μm) sections were cut with a Vibratome 1000 system (Davidson and Wallingford, 2005).

The imaging was performed with a Zeiss LSM5 Pascal confocal microscope. The images for bright field and fluorescence view were captured on a stereomicroscope (Leica MZ16FA). Cell height and nuclear position were measured with LSM5 Pascal software and cell surface area was measured with ImageProPlus software. Images used throughout this study have been enhanced using the Unsharp Mask filter in Adobe Photoshop.

Immunoblotting

Embryos were lysed in RIPA buffer (150 mM NaCl, 1% NP-40, 0.5% deoxycholate, 2 mM EDTA, 50 mM Tris, pH 8.0) containing protease inhibitors. After centrifugation, 10 μg supernatant was analyzed by SDS-PAGE and western blot assays were performed using standard protocols. Primary antibodies used were monoclonal anti-Myc antibody (1:2000 dilution, clone 9E10; Abcam), rabbit polyclonal anti-actin antibody (1:2000

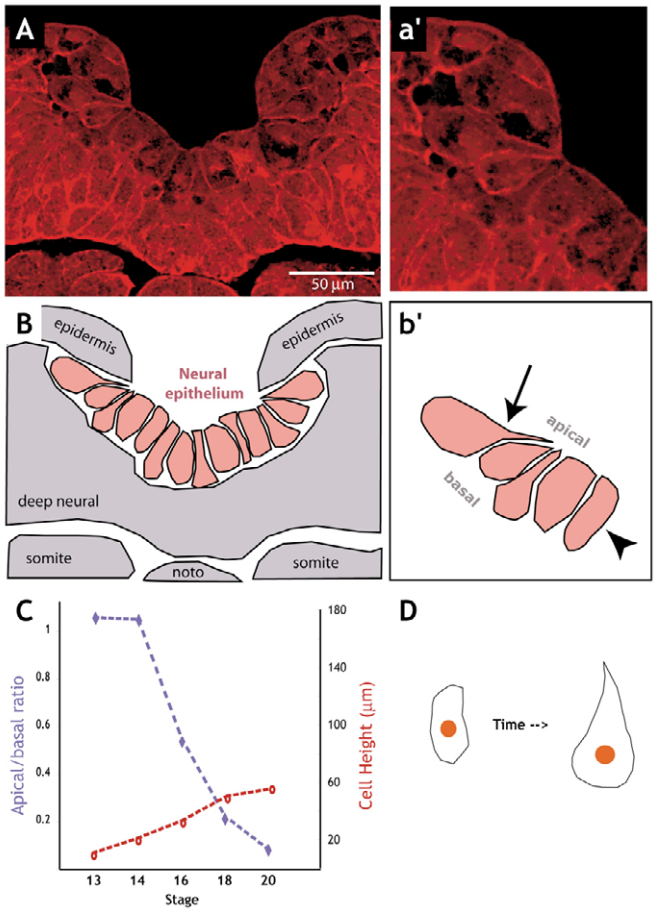

Fig. 1. Apical constriction and apicobasal cell elongation in the neural epithelium during neural tube closure. (**A**) Projection of confocal optical transverse sections through the anterior neural plate of neurulating *Xenopus* embryo. (**a′**) High-magnification view of a neural epithelial cell from A. (**B**) A schematic diagram of the section in A, illustrating the neural epithelial cells (red) and other surrounding tissues (grey). (**b′**) A schematic diagram of the section in a′. Cells in hingepoint regions constrict and elongate (arrow), cells in intermediate regions elongate, but constrict only a little (arrowhead). (**C**) Graph illustrating changes in apical constriction (blue; ratio of apical surface to basal surface measured from cross-sections) and apicobasal cell elongation (red; cell height in μm) of neuroepithelial cells during neural tube closure (stages 14-19; *n*=10 cells per stage). (**D**) Schematic illustrating the change in neural epithelial cell shape during neural tube closure.

dilution; Abcam) and rabbit polyclonal anti-γ-tubulin antibody (1:4000 dilution; Abcam). Horseradish peroxidase (HRP) signals were detected by SuperSignal West Pico Chemiluminescent Substrate (Pierce).

RESULTS

Shroom3 is required for both apical constriction and apicobasal cell elongation in the neural plate during neural tube closure

In developing *Xenopus* embryos, superficial neural epithelial cells undergo dramatic elongation and apical constriction during neural tube closure. The degree of apical constriction is discontinuous within this neural epithelium; certain cells constrict dramatically (Fig. 1A,a′,B,b′, arrow), whereas others increase their height, but constrict little (Fig. 1b′, arrowhead). The highly constricted cells are ordered in anteroposterior arrays of cells, called hingepoints, and the organization of these constricted cells is most easily seen by comparing cross-sections with the surface views (see Fig. S1 in the supplementary material). Examination of cross-sections at successive developmental stages revealed a progressive elongation and constriction of neuroepithelial cells over time (Fig. 1C,D). We observed that changes in cell height could occur independently of apical constriction. At the onset of neurulation (stages 13-14), cells of the neural plate almost doubled their height, from approximately 12 μm to approximately 22 μm, during a time when no apical constriction occurred (Fig. 1C).

Because Shroom3 induces apical constriction in neural epithelial cells (Haigo et al., 2003), we asked whether this protein was also involved in the control of cell elongation. We disrupted Shroom3 function using an antisense morpholino oligonucleotide (MO) that effectively blocks proper splicing of Shroom3; introduction of this MO results in translation of a non-functional Shroom3 protein and disrupts neural plate bending when injected into *Xenopus* embryos (Haigo et al., 2003).

Confocal imaging of cells within the neural plate revealed that embryos injected unilaterally with Shroom3 MO (morphants) develop with obvious defects in cell elongation on the injected side of the embryo (Fig. 2A,a′). Cell shape change progressed normally on the uninjected side of these embryos. Disruption of Shroom3 function by injection of the Shroom3-MO blocked apicobasal elongation of neural plate cells, such that the length of cells lacking Shroom3 function was approximately half that of control cells (Fig. 2B). By mid-neurulation, these cells are only as long as wild-type cells were at the onset of neurulation.

A failure of apical constriction in Shroom3 morphants was also apparent. Cells on the uninjected side of embryos took on the characteristic wedge shape, whereas cells on the injected side remained columnar (Fig. 2A,a′). We quantified apical constriction in the neural plate by measuring the apical surface area of neural cells in the robustly constricting hingepoint regions and also in the intermediate regions, where less constriction occurs (Fig. 2D,E). Apical surface areas in both regions were significantly increased in Shroom3 morphants (Fig. 2C).

To confirm our findings, we disrupted Shroom3 function using an alternative method. We showed previously that expression of the dominant-negative fragment Shroom3$^{754\text{-}1108}$ (DN-Shrm3) potently disrupts the activity of co-expressed Shroom3 in an in vitro assay (Haigo et al., 2003). When we expressed DN-Shrm3 in neural epithelial cells, we observed clear defects in apicobasal cell elongation, similar to that observed in Shroom3 morphants. In addition, expression of DN-Shrm3 reduced apical constriction and cell elongation throughout the neural plate to a degree comparable to the Shroom3-MO (Fig. S2c′ in the supplementary material). These results demonstrate that Shroom3 is required for apicobasal cell elongation in neural epithelial cells in addition to its role in apical constriction.

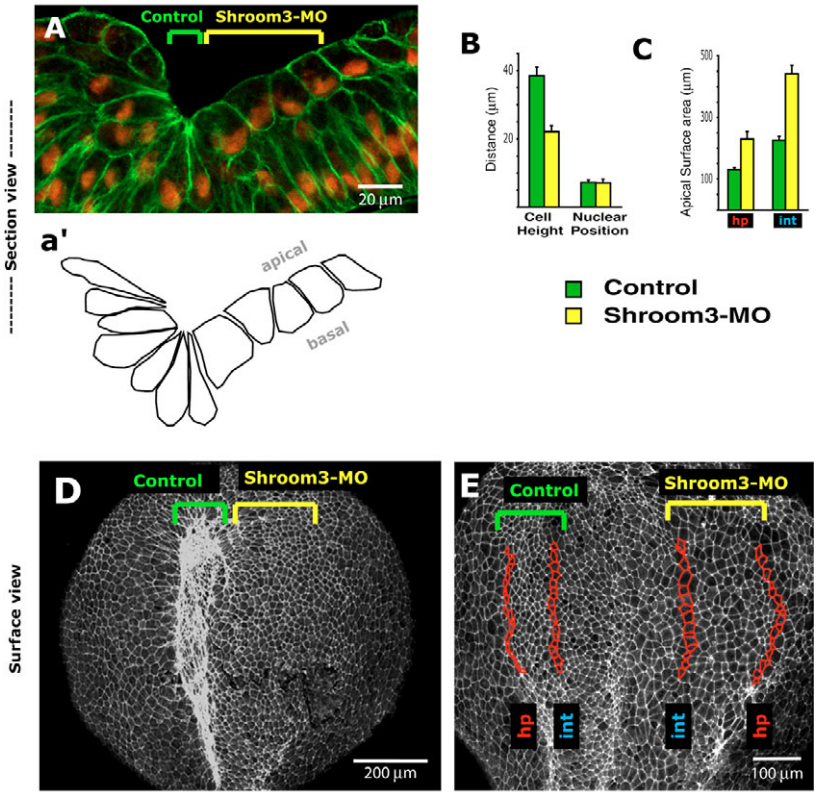

Fig. 2. Shroom3 is required for apical constriction and apicobasal cell elongation in neural epithelial cells during neural tube closure. (**A**) Cross-section through the closing anterior neural tube of an embryo injected on one side with Shroom3-MO. Anti-α-tubulin staining reveals cell cortices and DAPI reveals nuclei. (**a′**) Schematic of neuroepithelial cell shape in A. (**B**) Graph of apicobasal cell height and the distance between the basal cell surface and the basal limit of the nucleus for hingepoint cells in control and Shroom3-MO-injected regions at stage 18 (mean ± s.e.m.; ctl, *n*=12; Mo, *n*=11). (**C**) Graph of apical cell surface areas of control and Shroom3-MO-injected sides of fixed embryos in hingepoint (hp) and intermediate (int) regions of fixed embryos at stage 18 (mean ± s.e.m.; *n*=25). Hingepoint and intermediate regions are defined in Fig. S1 in the supplementary material. (**D**) Dorsal projection of stage 18 embryo to visualize apical cell surface areas. (**E**) Dorsal projection of stage 16 *Xenopus* embryo stained with phalloidin to visualize cell shapes. Cells defined as the hp and int regions are indicated by red outlines and labeled at the bottom of the panel (see also Fig. S1 in the supplementary material). Embryo has been injected on one side with Shroom3-MO.

Shroom3 is required for the assembly of parallel MT arrays in the apical region of neural epithelial cells

We next pursued the mechanism by which Shroom3 mediates changes in cell length. Like most epithelia, neural epithelial cells contain parallel arrays of MTs aligned along their apicobasal axis, and increasing cell height is associated with the assembly of a much more dense array of these aligned MTs (Burnside, 1973; Karfunkel, 1971). We examined MTs using confocal microscopy and an antibody against α-tubulin. Apical MT arrays were readily apparent in wedging neuroepithelial cells (Fig. 3A,a′). We observed thick, parallel arrays of MTs emanating from the apical cell surface and extending through approximately the apical third of the cell (Fig. 3A,a′), consistent with previous electron microscopy studies in *Xenopus* (Karfunkel, 1971).

Strikingly, the failure of cell elongation in Shroom3 morphants was uniformly associated with a failure to assemble the thick, aligned MT arrays in the apical region (Fig. 3B,b′). Identical results were observed following expression of the dominant-negative fragment DN-Shrm3 (Fig. S2C,c′ in the supplementary material). In contrast to the parallel MT arrays, overall MT assembly was not disrupted in cells lacking Shroom3 function. Cortical and perinuclear MT networks appeared similar in both control cells and in cells lacking Shroom3 function (Fig. 3A,B). These data suggest that Shroom3 directs the assembly of a discrete population of aligned MTs and are consistent with the notion that such MTs drive changes in cell height during neural tube closure.

Finally, we observed that the failure of MT organization and the failure of cell shape change in Shroom3 morphants did not stem from general defects in apicobasal cell polarity. First, we observed that in Shroom3 morphants, nuclear positioning was highly uniform (Fig. 2A) and the position of nuclei relative to the basal cell surface was identical to that in normal neural cells (Fig. 2B). These findings are consistent with the normal appearance of perinuclear MTs in Shroom3 morphants (Fig. 3A,B). Second, we found that apical markers were maintained in the absence of Shroom3 function. For example, in control embryos, ZO-1 and Par3 were tightly localized at apical cell-cell junctions of elongating neural plate cells (Fig. 3C and data not shown). In Shroom3 morphants, ZO-1 and Par3 remained localized normally, even in cells that lacked robust apicobasal MT arrays and that failed to constrict and elongate (Fig. 3D and data not shown).

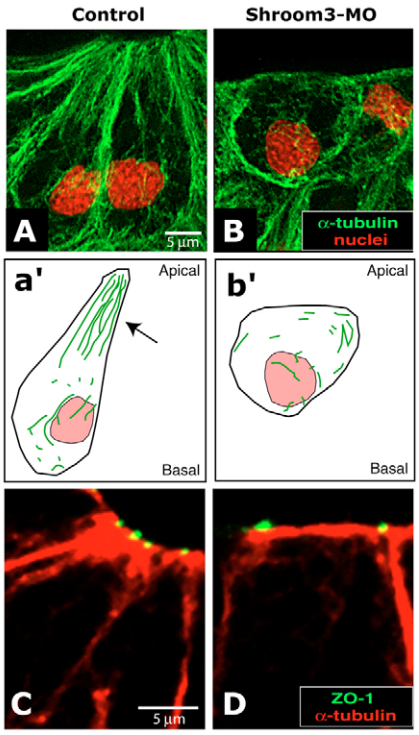

Fig. 3. Shroom3 is required for assembly of discrete arrays of parallel MTs in elongating neural epithelial cells. (**A**) High-magnification view of MTs in control hingepoint cells (green, anti-α-tubulin; red, propidium iodide, nuclei). (**a′**) Schematic of a cell shown in A. Arrow indicates parallel MT arrays. (**B**) High-magnification view of MTs in dorsolateral hingepoint (DLHP) cells lacking Shroom3 function. (**b′**) Schematic of a cell shown in B. (**C**) High-magnification view of control hingepoint cells (green, ZO-1; red, anti-α-tubulin). (**D**) High-magnification view of hingepoint cells lacking Shroom3 function. Shape changes are eliminated, but ZO-1 remains apically localized at cell-cell junctions.

Cell elongation and assembly of apical MT arrays are associated with Shroom3-dependent redistribution of γ-tubulin in neural epithelial cells

To begin to characterize the molecular basis of MT organization in the developing neural plate, we examined the distribution of γ-tubulin in the neural epithelium by immunohistochemistry. In many epithelial cell types, centrosome-like foci of γ-tubulin are observed near the apical cell surface, from which MTs are thought to be organized (Meads and Schroer, 1995; Müsch, 2004; Rizzolo and Joshi, 1993).

By contrast, we observed that in neural plate cells γ-tubulin was distributed as a thick cloud with many brighter foci per cell (Fig. 4A,B). This broad accumulation of γ-tubulin filled approximately the apical third of each elongating neural plate cell during neural tube closure, thus correlating in time and space with the assembly of the robust apicobasally aligned MT arrays described above (Fig. 4A,a′). γ-tubulin accumulated apically at the early neurula stages, prior to the onset of robust apical constriction (stage 16; Fig. S2A,B in the supplementary material), demonstrating that the apical concentration of γ-tubulin was not a function of the constricting apical surface of neuroepithelial cells. We obtained identical results with two different γ-tubulin antibodies (data not shown).

The broad, intense distribution of γ-tubulin throughout the apical region of neural plate cells was unexpected, and, to our knowledge, such a distribution in interphase epithelial cells has not been previously reported. To ask whether this unique redistribution of γ-tubulin could be mediated by Shroom3, we examined neural epithelial cells after the completion of neural tube closure, when Shroom3 expression is rapidly downregulated (Haigo et al., 2003). We found that after neural tube closure was complete, our γ-tubulin antibody detected centrosome-like foci at the apical cell surface (Fig. 4C,c′,D), similar to that described for mature mammalian neuroepithelial cells (Chenn et al., 1998). These data suggest that the broad apical accumulation of γ-tubulin may result directly from the action of Shroom3.

In light of these findings, we asked whether loss of Shroom3 function affected the apical accumulation of γ-tubulin. We observed that injection of the Shroom3-MO completely eliminated the accumulation of γ-tubulin in the neural plate, coincident with the failure of cells to form aligned MT arrays and to elongate (Fig. 4E,e′). To confirm this result, we expressed the DN-Shrm3 fragment. As was the case for morphants, cells expressing DN-

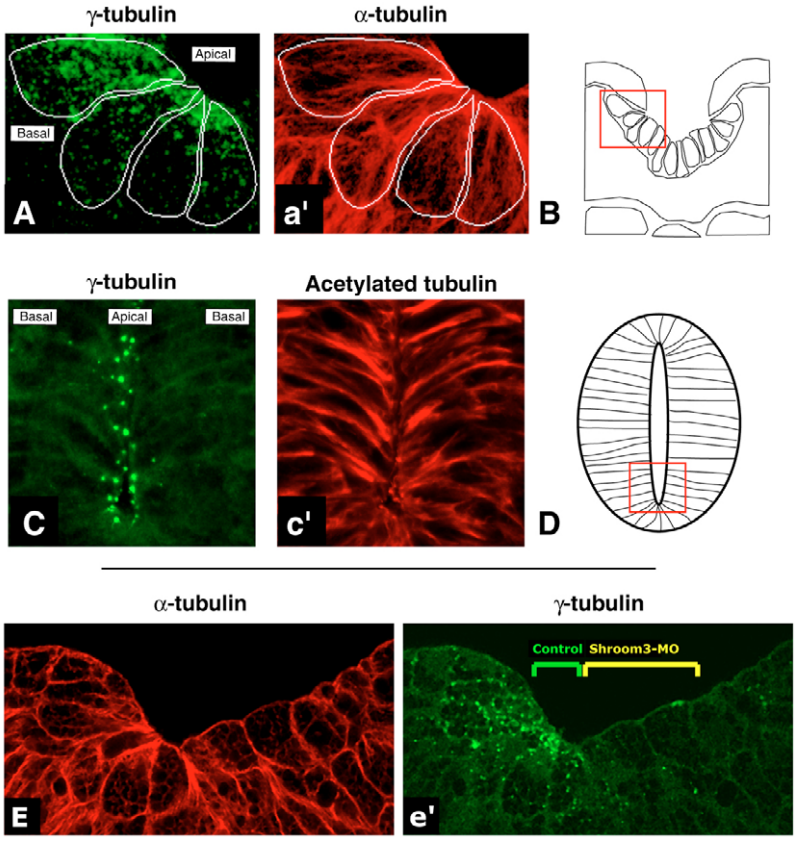

Fig. 4. Shroom3 controls the distribution of γ-tubulin in neuroepithelial cells during neural tube closure. (**A**) High-magnification projection of a stack of optical sections showing elongating neural epithelial cells stained for γ-tubulin (white lines indicate cell outline). (**a′**) α-tubulin staining for cells shown in A. (**B**) Schematic of the closing neural tube indicating location of section shown in A (red box). (**C**) γ-tubulin staining in a projection of optical sections reveals centrosome-like foci at the apical surfaces of mature neuroepithelial cells. (**c′**) Acetylated-α-tubulin staining reveals cell outlines in the ventral region of the closed *Xenopus* neural tube. (**D**) Schematic of the neural tube indicating location of section shown in C (red box). (**E**) Optical section showing α-tubulin in an embryo unilaterally injected with Shroom3-MO (right side is injected, left side is control). (**e′**) γ-tubulin staining for cells shown in E.

Shrm3 also failed to accumulate γ-tubulin apically (Fig. S2C in the supplementary material). Western blotting revealed that the total levels of γ-tubulin in the dorsal tissues of Shroom3-MO-injected embryos were not affected (Fig. S3A in the supplementary material), suggesting that Shroom3 directs a redistribution of γ-tubulin in apical regions of neuroepithelial cells.

Shroom3 is sufficient to elicit apicobasal cell elongation in naïve epithelial cells

To further explore the activity of Shroom3, we took advantage of our previously described gain-of-function assay using the epithelial cells that surround the cleavage-stage *Xenopus* embryo (Fig. 5A). These cells (the superficial blastomeres) provide an excellent source of naïve epithelial cells in which to test protein function (see Dollar et al., 2005; Haigo et al., 2003). Such cells display a robust apicobasal polarity characteristic of epithelial cells (Chalmers et al., 2005; Roberts et al., 1992) and are transcriptionally quiescent, such that the effects of injected mRNAs represent the direct action of the protein encoded by that mRNA.

Because neural cells lacking Shroom3 function failed to elongate, we first asked whether ectopic Shroom3 was sufficient to induce apicobasal elongation in naïve cells. We injected *Shroom3* mRNA into *Xenopus* embryos and reared them to blastomere stages, stained them with phalloidin to detect apical actin accumulation [indicating the presence of functional Shroom3 protein (see Haigo et al., 2003)] and measured the apicobasal length of these cells. Indeed, Shroom3-expressing cells dramatically increased their height when compared with neighboring cells lacking Shroom3 or when compared with

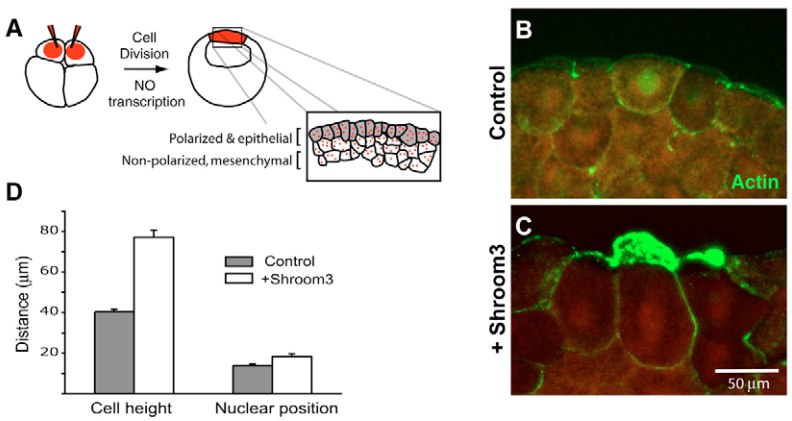

Fig. 5. Shroom3 is sufficient to drive apicobasal cell elongation in naïve epithelial cells. (**A**) Schematic depicting the epithelial character of the superficial blastomeres in *Xenopus* (see also Chalmers et al., 2005; Dollar et al., 2005; Haigo et al., 2003; Roberts et al., 1992). (**B**) Cross-section through superficial blastomeres of a control embryo. Phalloidin staining reveals cell cortices (green) and propidium iodide reveals nuclei (red). (**C**) Cross-section through superficial blastomeres of an embryo ectopically expressing Shroom3. Cells with accumulated apical actin also display increased cell height. (**D**) Graph of apicobasal cell height and the distance between the basal cell surface and the basal limit of the nucleus for superficial blastomeres in control and Shroom3-injected regions (mean ± s.e.m.; ctl, *n*=26; Shroom3, *n*=19).

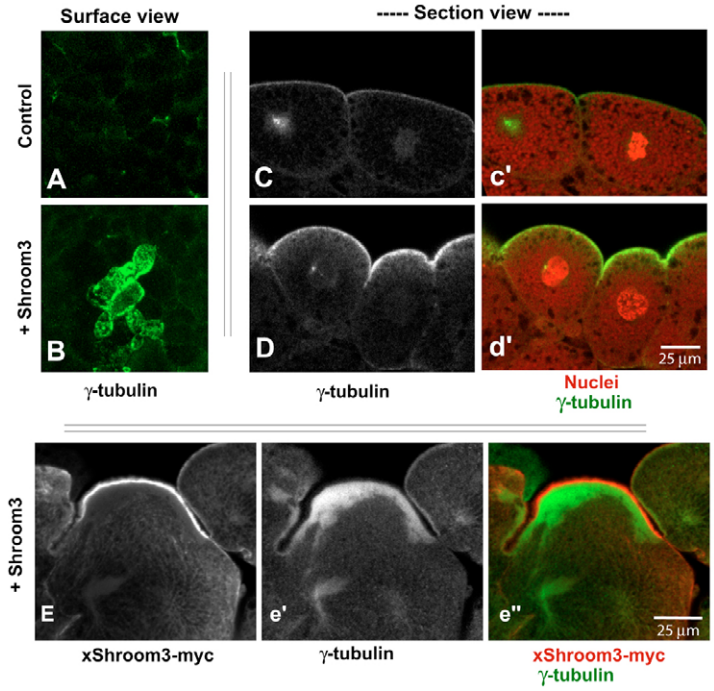

Fig. 6. Shroom3 is sufficient to drive apical accumulation of γ-tubulin in naïve epithelial cells. (**A**) Control embryo showing surface view of the superficial blastomere epithelium stained with anti-γ-tubulin. (**B**) Shroom3-expressing embryo showing surface view of the superficial blastomere epithelium stained with anti-γ-tubulin. (**C**) Cross-section through superficial blastomeres of a control embryo at early stages stained with anti-γ-tubulin. Merged image is shown in **c′** (green, γ-tubulin; red, propidium iodide). (**D**) Cross-section through superficial blastomeres of an embryo ectopically expressing Shroom3 at early stages stained for anti-γ-tubulin. Merged image is shown in **d′** (green, γ-tubulin; red, propidium iodide). (**E**) Cross-section through superficial blastomeres of an embryo ectopically expressing Shroom3 at later stages. Embryo has been stained to detect Myc-Shroom3 (E; red) and γ-tubulin (**e′**; green). Merged image is shown in **e″**.

cells in similar regions of uninjected embryos (Fig. 5B-D). Thus, in addition to its role in governing apical constriction, Shroom3 is also both necessary and sufficient to induce apicobasal cell elongation.

Shroom3 directs apical accumulation of γ-tubulin in naïve epithelial cells

Our data in the neural epithelium suggest that the effect of Shroom3 on cell elongation stems from a relocalization of γ-tubulin (Fig. 4). To explore this hypothesis further, we again took advantage of the naïve epithelial cells that surround the cleavage-stage *Xenopus* embryo (see Fig. 5A). Ectopic expression of Shroom3 resulted in a dramatic accumulation of γ-tubulin at apical cell surfaces (Fig. 6). At early stages, prior to a change in cell shape, the accumulated γ-tubulin in Shroom3-expressing cells localized tightly to the apical cell surface (Fig. 6D,d′). At later stages, when Shroom3-expressing cells have assumed a wedge shape and have increased their height, a broader, more diffuse accumulation of γ-tubulin was observed throughout the apical region of the cells (Fig. 6E,e′,e″).

Consistent with our data from loss-of-function manipulations, western blotting demonstrated that the accumulation of γ-tubulin in naïve cells expressing Shroom3 was not associated with a change in the total amount of γ-tubulin present (Fig. S3B in the supplementary material). These findings therefore suggest that Shroom3 acts to alter the spatial distribution, rather than absolute levels, of γ-tubulin in epithelial cells. Moreover, we found that the ectopically expressed Shroom3 protein did not colocalize with γ-tubulin, but instead occupies a domain immediately apical to the region of accumulated γ-tubulin (Fig. 6E,e′,e″). Consistent with the localization data, co-immunoprecipitation experiments failed to detect a physical interaction between Shroom3 and γ-tubulin (data not shown).

Together with our loss-of-function data (Fig. 4, and see above), these results demonstrate that Shroom3 is not only necessary but also sufficient to drive apical redistribution of γ-tubulin in epithelial cells. We suggest that this effect on γ-tubulin localization underlies the capacity of Shroom3 to organize apicobasal MT arrays and drive apicobasal cell elongation.

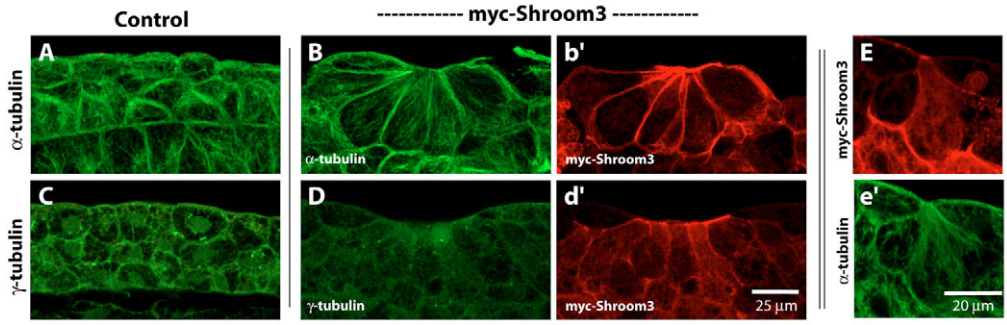

Fig. 7. Expression of Shroom3 in epidermal cells recapitulates the events underlying neuroepithelial cell shape change. (**A**) Control epidermis stained for α-tubulin. (**B**) Epidermis expressing Shroom3 stained for α-tubulin. Cells expressing Shroom3 (marked by anti-Myc; **b′**) constrict and elongate. Parallel arrays of MTs emanate from the apical cell surface. (**C**) Control epidermis stained for γ-tubulin. (**D**) Epidermis expressing Shroom3 stained for γ-tubulin. Cells expressing Shroom3 in this panel (marked by anti-Myc, red; **d′**) are only slightly constricted, but are elongated and contain a broad, diffuse accumulation of γ-tubulin. (**E**) A single epidermis cell expressing high levels of Shroom3 apically constricts and also elongates. (**e′**) Anti-α-tubulin staining of the cell shown in E.

Expression of Shroom3 is sufficient to drive assembly of apicobasally aligned MTs in epithelial cells

Expression of Shroom3 in blastomeres recapitulates many features of neuroepithelial cell shape change, including actin accumulation, apical constriction, cell elongation and γ-tubulin accumulation. However, the very dense yolk of *Xenopus* blastomeres significantly hinders imaging of MTs. To analyze the result of Shroom3 gain-of-function on the MT cytoskeleton, we used plasmid DNA injections into early embryos to mosaically express Myc-tagged Shroom3 in the mature epidermis (see Vize et al., 1991).

Compared with control epidermal cells, Shroom3-expressing cells apically constrict and elongate dramatically (Fig. 7A,B,b′). Importantly, the elongation is associated with assembly of robust MT arrays emanating from the apical surface (Fig. 7B). Finally, as in neural epithelial cells, Shroom3-expressing epidermal cells develop a broad, diffuse accumulation of γ-tubulin that is associated with MT assembly and cell elongation (Fig. 7C,D,d′). As is the case for normal neural plate cells, accumulation of γ-tubulin in Shroom3-expresssing epidermal cells was associated with cell elongation even in cells that have yet to fully constrict their apical surface (compare Fig. 7D,d′ with Fig. S2A,a′ in the supplementary material). Thus, expression of Shroom3 in epidermal cells recapitulates with remarkable accuracy the cell shape changes and the underlying subcellular events observed in hingepoint cells in the neural epithelium.

Shroom3-mediated elongation occurs cell-autonomously

It is possible that Shroom3 drives elongation cell-autonomously, but it is also possible that elongation is a by-product of Shroom3-mediated changes in overall tissue geometry. To address this question, we again examined embryos mosaically expressing Shroom3 in the epidermis. We found many cases in which single epidermal cells expressed Shroom3 and were surrounded by non-expressing epidermal cells. In all cases, individual, isolated Shroom3-expressing cells were apically constricted and significantly elongated in the apicobasal axis (Fig. 7E,e′). This result demonstrates that cell elongation mediated by Shroom3 is cell autonomous and is consistent with a previous finding that elongation is cell-autonomous in neural epithelial cells (Holtfreter, 1946).

Joint control of γ-tubulin and actin distribution by Shroom3

Shroom3 could directly impact both MT and actin assembly, or alternatively, one of the effects could be secondary to the other. The uncoupling of cell elongation from apical constriction in neural cells (Fig. 1C) raises the possibility that Shroom3 may independently control actin- and MT-based cell shape changes.

To begin to probe this possibility, we turned again to our gain-of-function assay using naïve blastomeres (see Fig. 5A). We reasoned that if one activity was primary and the other secondary, then such would be reflected in the timing of actin and γ-tubulin accumulation at the apical surface. When we expressed Shroom3 by mRNA injection at the four-cell stage, we observed simultaneous accumulation of γ-tubulin and actin at the apical cell surface within less than 1 hour (Fig. 8A,B). In no case did we observe apical accumulation of one component prior to that of the other.

Moreover, the patterns of accumulated γ-tubulin and actin at the apical surfaces of Shroom3-expressing cells also argued that their accumulation was not strictly interdependent. Some cells that accumulated large amounts of γ-tubulin did not accumulate actin (Fig. 8D,d′,d″, bracket), and conversely some cells that accumulated high levels of actin failed to accumulate significant amounts of γ-tubulin (Fig. 8D,d′,d″, arrow).

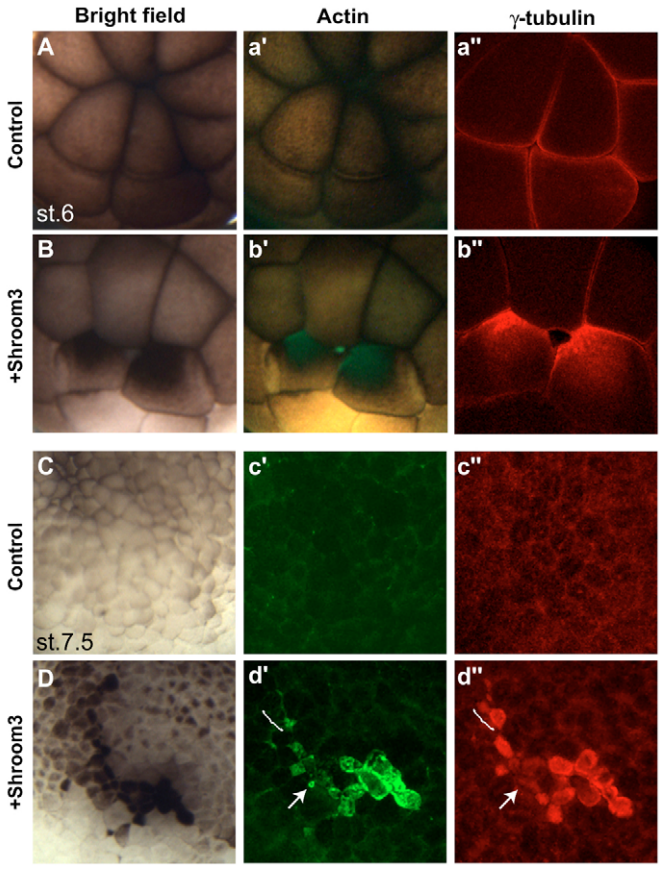

Fig. 8. Shroom3 coordinates the polarized assembly of both actin and γ-tubulin cytoskeletons. (**A**) Control embryo at stage 6 showing surface view of the superficial blastomere epithelium stained with phalloidin (**a′**) and anti-γ-tubulin (**a″**). (**B**) Shroom3-expressing embryo at stage 6 showing surface view of the superficial blastomere epithelium stained with phalloidin (**b′**) and anti-γ-tubulin (**b″**). (**C**) Control embryo at stage 7.5 showing surface view of the superficial blastomere epithelium stained with phalloidin (**c′**) and anti-γ-tubulin (**c″**). (**D**) Shroom3-expressing embryo at stage 7.5 showing surface view of the superficial blastomere epithelium stained with phalloidin (**d′**) and anti-γ-tubulin (**d″**). Bracket indicates accumulated γ-tubulin with little actin; arrow indicates accumulated actin with little γ-tubulin.

Shroom family proteins are associated with MT-based elongation and accumulation of γ-tubulin in non-neural epithelial cells

The *Xenopus*, mouse and human genomes each contain additional proteins that are closely related in sequence to Shroom3 (Hagens et al., 2006). Previous reports have associated each of these proteins with the actin cytoskeleton, but our data above demonstrate that Shroom3 can coordinate the response of both MT and actin cytoskeletons to induce diverse cell shape changes. To ask whether MT-regulating activity is a conserved feature of this protein family, we studied the related protein Shroom1 (Hagens et al., 2006; Staub et al., 1992).

In situ hybridization revealed that both Shroom3 and Shroom1 were expressed in epithelial cells of the cement gland (Fig. 9A,B), an adhesive organ of amphibian embryos (Perry and Waddington, 1966).

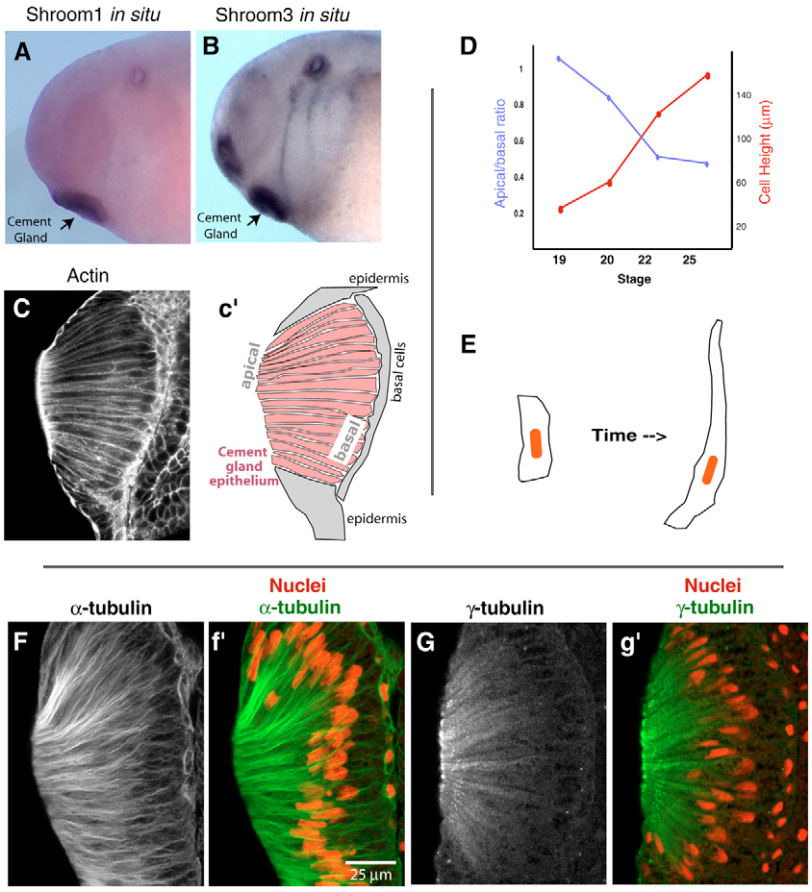

Fig. 9. Shroom family proteins and cell elongation in non-neural cells. (**A**) In situ hybridization reveals Shroom1 expression in the cement gland. (**B**) In situ hybridization reveals Shroom3 expression in the cement gland, and also the invaginating nasal and otic placodes. (**C**) Cross-section through the cement gland, stained with phalloidin to reveal cell shapes. (**c′**) A schematic diagram of the section in C, illustrating the cement gland epithelial cells (red) and other surrounding tissues (grey). (**D**) Graph of changes in apical constriction (blue) and apicobasal cell elongation (red) of cement gland cells over time (stages 19-25). (**E**) A schematic diagram illustrating the change in cement gland epithelial cell shape. (**F**) Projection of optical sections of α-tubulin staining of cement gland epithelial cells. (**f′**) α-tubulin staining shown in F merged with propidium iodide staining to show nuclei. (**G**) Robust apical MT arrays in the cement gland are associated with a broad apical accumulation of γ-tubulin. (**g′**) γ-tubulin staining shown in G merged with propidium iodide staining to show nuclei.

This strong expression was intriguing because these cells undergo a radical apicobasal elongation, but constrict only slightly (Fig. 9C-E). As in neural cells, cement gland cells undergo periods in which cell elongation occurs independently of apical constriction; indeed, cells increased their height by over 30 μm during a time when apical constriction was negligible (see stages 22-25 in Fig. 9D).

Consistent with a role for Shroom1 and Shroom3 in MT-mediated cell elongation, cement gland cells contain robust arrays of apicobasally aligned MTs that emanate from the apical cell surface (Fig. 9F,f′) (Perry and Waddington, 1966; Picard, 1976). Moreover, the thick arrays of MTs in the cement gland were again correlated in time and space with a broad, intense accumulation of γ-tubulin throughout the apical regions of these cells (Fig. 9F,G,g′).

We next tested the activity of Shroom1 using our naïve blastomere assay system (see Fig. 5A). Unlike Shroom3, expression of Shroom1 failed to elicit apical accumulation of actin microfilaments and did not induce apical constriction (data not shown). Nonetheless, ectopic expression of Shroom1 did elicit apical accumulation of γ-tubulin in naïve epithelial cells (Fig. 10A,B,b′), consistent with a role for Shroom1 in governing MT architecture. Interestingly, whereas Shroom3 drove accumulation of γ-tubulin across the apical cell surface, Shroom1 drove accumulation of γ-tubulin specifically at cell-cell junctions.

DISCUSSION

Shroom family proteins influence both MT and actin cytoskeletons

Cell shape changes make an important contribution to morphogenetic tissue movements. Two such cell shape changes include apical constriction and apicobasal cell elongation. Previously, we demonstrated that Shroom3 is necessary and sufficient to induce apical constriction and coincident apical actin accumulation (Haigo et al., 2003). We now demonstrate a novel, additional function for Shroom3 in the control of MT-mediated cell shape changes during neural tube closure. We show that Shroom3 is necessary and sufficient to induce an apical redistribution of γ-tubulin, the assembly of robust apicobasal MT arrays, and apicobasal cell elongation in epithelial cells. Shroom3 is a member of a small family of proteins, all of which have been associated in some way with the actin cytoskeleton (Dietz et al., 2006; Hagens et al., 2006; Hagens et al., 2005; Haigo et al., 2003; Hildebrand, 2005; Prat et al., 1996; Yoder and Hildebrand, 2006). In this study, we show that another member of this family, Shroom1, is also associated with cell elongation and can drive apical redistribution of γ-tubulin in naïve epithelial cells.

The mechanisms by which Shroom family proteins function remain obscure, but it was shown recently that Shroom3 drives the apical localization of myosin II in both cultured cells and in the mouse neural plate, and that myosin II function is essential for Shroom3-mediated apical constriction in naïve cells (Hildebrand, 2005). How this actin-myosin system is linked with γ-tubulin accumulation is not yet clear, but there is evidence to suggest that these effects are at least partially independent of one another. For example, in Shroom3-expressing blastomeres, actin and γ-tubulin can accumulate independently (Fig. 8). Moreover, Shroom1 and also another family member, Shroom2, can each drive apical accumulation of γ-tubulin, but neither can elicit significant actin assembly or apical constriction (Fig. 10A) (Fairbank et al., 2006). Finally, Shroom3 drives both apical constriction and cell elongation, and these two cell shape changes can occur independently in both

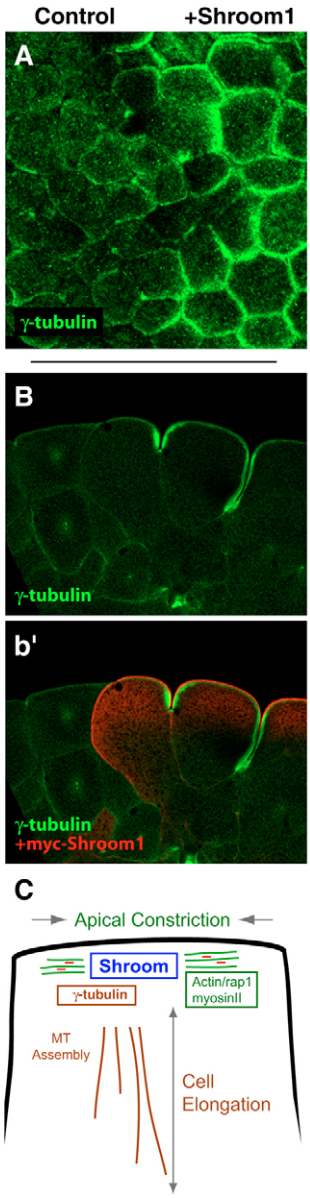

Fig. 10. Shroom1 expression is sufficient to elicit apical accumulation of γ-tubulin in naïve epithelial cells. (**A**) Surface view of blastomeres stained for γ-tubulin. Shroom1-expressing cells (right) accumulate high levels of γ-tubulin at cell-cell junctions. (**B**) Section view of blastomeres stained for γ-tubulin. (**b′**) Shroom1-expressing cells [indicated by anti-Myc staining (red)] accumulate excess γ-tubulin at cell-cell boundaries. (**C**) Model for Shroom3-mediated cell shape changes in neural epithelial cells. Model is based on data from the current work and also on the work of Hildebrand (Hildebrand, 2005) and Haigo et al. (Haigo et al., 2003).

neural and cement gland epithelial cells (Fig. 1C; Fig. 9D). Combining our data with that of others (e.g. Hildebrand, 2005), we propose a preliminary model whereby apically localized Shroom3 directs accumulation of both actomyosin and γ-tubulin, thus affecting both apical constriction and apicobasal cell heightening (Fig. 10C).

Finally, the role played by γ-tubulin during Shroom3-mediated cell elongation remains to be discovered. The broad distribution of γ-tubulin in elongating neural epithelial cells has not to our knowledge been reported in non-mitotic cells, but it is reminiscent of γ-tubulin distribution in mitotic spindles (Lajoie-Mazenc et al., 1994). In interphase cells, γ-tubulin is generally associated with MT minus-ends, but in the mitotic spindle it associates with the sides of MTs (Gunawardane et al., 2000; Lajoie-Mazenc et al., 1994). It will be important in the future to determine how γ-tubulin interacts with the MTs that elongate neural epithelial cells and how Shroom proteins regulate the distribution of γ-tubulin. Specific proteins, such as GCP-WD, are known to regulate γ-tubulin targeting during mitosis (Luders et al., 2006), so it is tempting to speculate that similar proteins mediate Shroom-dependent γ-tubulin redistribution.

Common mechanisms of apical constriction in vertebrates and invertebrates

How conserved is the mechanism of cell shape change across evolutionarily diverse cell types? Apical localization and contraction of actin and myosin appear to be universal, driving apical constriction in *Volvox*, *Drosophila*, *Caenorhabditis elegans* and vertebrates (Hildebrand, 2005; Lee and Goldstein, 2003; Nance and Priess, 2002; Nishii and Ogihara, 1999; Young et al., 1993). Likewise, an increase in cell length is observed in apically constricting cells across taxa, including *Volvox*, *Drosophila*, shrimps, sand dollars, mice, chicks and frogs (Burnside, 1973; Hertzler and Clark, Jr, 1992; Kam et al., 1991; Kominami and Takata, 2000; Nishii and Ogihara, 1999; Schoenwolf and Franks, 1984; Schroeder, 1970; Sweeton et al., 1991; Viamontes and Kirk, 1977).

We have shown here that Shroom3 governs both apicobasal elongation and apical constriction by organizing both MTs and actin. Recent studies likewise implicate a single molecule in the governance of these two cell shape events in *Drosophila*. An exchange factor for the small GTPase Rho, DRhoGEF2, appears to be both necessary and sufficient to induce apical constriction and cell elongation (Barrett et al., 1997; Hacker and Perrimon, 1998; Nikolaidou and Barrett, 2004; Rogers et al., 2004). Like Shroom3, this molecule is implicated in not only myosin II localization, but also in MT organization, in this case through localization of the MT plus-end-associated protein EB1 (Dawes-Hoang et al., 2005; Rogers et al., 2004). A very close linkage of MT and actin organization, in some cases by a single molecule, thus appears to underlie the almost ubiquitous coincidence of cell heightening and apical constriction.

Although such unifying features are important, several discrepancies must be noted. For example, apical constriction in the roundworm is not apparently associated with apicobasal cell heightening (Lee and Goldstein, 2003; Nance and Priess, 2002). Moreover, Shroom3 controls the apical accumulation of γ-tubulin, a MT minus-end-associated protein (Figs 4, 6), whereas DRhoGEF2 directs the apical localization of EB1, a plus-end binding protein (Rogers et al., 2004). Finally, the crucial role for a RhoGEF in *Drosophila* is perhaps surprising given that dominant-negative Rho constructs clearly cannot block Shroom-mediated apical constriction (Haigo et al., 2003; Hildebrand, 2005). In fact, the opposite appears to be true, as it is loss of a RhoGAP, rather than a RhoGEF, that disrupts apical constriction in vertebrates (Brouns et al., 2000). An understanding of such discrepancies will be required before a comprehensive picture of these cell shape changes will be brought into focus.

Cell polarity in developing epithelia

One interesting implication of the results in this study concerns the nature of cell polarity within epithelia during morphogenesis. Unlike most epithelia, we find that in neural plate cells engaged in apical

constriction, γ-tubulin is not tightly associated with the apical cell membrane, nor is it localized in centrosome-like foci at the apical surface. Instead, we find that γ-tubulin accumulates in a broad distribution throughout the apical region of elongating neural epithelial cells (Fig. 4). This odd distribution of γ-tubulin is coincident with expression of Shroom3, and a similar γ-tubulin distribution was observed in Shroom1-expressing cells in the *Xenopus* cement gland (Fig. 9).

This distribution of γ-tubulin may reflect the partial downregulation of apicobasal polarity previously reported for neural epithelial cells during neural tube closure: whereas some polarity markers remain apically localized during neural tube closure, others do not (Aaku-Saraste et al., 1996; Aaku-Saraste et al., 1997). These findings suggest that cytoskeletal elements maintaining overall cell polarity can be uncoupled from those elements driving cell shape change. This interpretation is consistent with our findings that whereas both actin- and MT-based cell shape changes are disrupted in embryos lacking Shroom3 function, ZO-1 and Par3 remain apically localized (Fig. 3). In sum, our data suggest that Shroom family proteins play a central role in controlling the assembly of discrete cytoskeletal elements that drive cell shape changes in developing epithelia. Moreover, we suggest that partial depolarization may be a common mechanism underlying morphogenetic events involving epithelial sheets.

We thank P. Fairbank, E. Kieserman and A. Ellis for technical assistance, J. Sisson for critical insights, and A. Ewald, J. Gross, J. Hildebrand and S. Haigo for helpful discussions and reading of the manuscript. We thank the Kirschner laboratory for the gift of *Xenopus* γ-tubulin antibody. This work was supported by a UT Austin/University Co-op Undergraduate Research Fellowship to H.M.S., a Career Award in the Biomedical Sciences from the Burroughs Wellcome Fund to J.B.W. and by the NIH/NIGMS (1RO1GM74104).

Supplementary material

Supplementary material for this article is available at http://dev.biologists.org/cgi/content/full/134/7/1431/DC1

References

Aaku-Saraste, E., Hellwig, A. and Huttner, W. B. (1996). Loss of occludin and functional tight junctions, but not ZO-1, during neural tube closure – remodeling of the neuroepithelium prior to neurogenesis. *Dev. Biol.* **180**, 664-679.

Aaku-Saraste, E., Oback, B., Hellwig, A. and Huttner, W. B. (1997). Neuroepithelial cells downregulate their plasma membrane polarity prior to neural tube closure and neurogenesis. *Mech. Dev.* **69**, 71-81.

Bacallao, R., Antony, C., Dotti, C., Karsenti, E., Stelzer, E. H. and Simons, K. (1989). The subcellular organization of Madin-Darby canine kidney cells during the formation of a polarized epithelium. *J. Cell Biol.* **109**, 2817-2832.

Barrett, K., Leptin, M. and Settleman, J. (1997). The Rho GTPase and a putative RhoGEF mediate a signaling pathway for the cell shape changes in Drosophila gastrulation. *Cell* **91**, 905-915.

Bre, M. H., Pepperkok, R., Hill, A. M., Levilliers, N., Ansorge, W., Stelzer, E. H. and Karsenti, E. (1990). Regulation of microtubule dynamics and nucleation during polarization in MDCK II cells. *J. Cell Biol.* **111**, 3013-3021.

Brouns, M. R., Matheson, S. F., Hu, K. Q., Delalle, I., Caviness, V. S., Silver, J., Bronson, R. T. and Settleman, J. (2000). The adhesion signaling molecule p190 RhoGAP is required for morphogenetic processes in neural development. *Development* **127**, 4891-4903.

Brun, R. B. and Garson, J. A. (1983). Neurulation in the Mexican salamander (Ambystoma mexicanum): a drug study and cell shape analysis of the epidermis and the neural plate. *J. Embryol. Exp. Morphol.* **74**, 275-295.

Burnside, B. (1973). Microtubules and microfilaments in amphibian neurulation. *Am. Zool.* **13**, 989-1006.

Chalmers, A. D., Pambos, M., Mason, J., Lang, S., Wylie, C. and Papalopulu, N. (2005). aPKC, Crumbs3 and Lgl2 control apicobasal polarity in early vertebrate development. *Development* **132**, 977-986.

Chenn, A., Zhang, Y. A., Chang, B. T. and McConnell, S. K. (1998). Intrinsic polarity of mammalian neuroepithelial cells. *Mol. Cell. Neurosci.* **11**, 183-193.

Davidson, L. A. and Wallingford, J. B. (2005). Visualizing morphogenesis in frog embryos. In *Imaging in Neuroscience and Development* (ed. R. Yuste and A. Konnerth), pp. 125-136. Cold Spring Harbor, NY: Cold Spring Harbor Laboratory Press.

Dawes-Hoang, R. E., Parmar, K. M., Christiansen, A. E., Phelps, C. B., Brand, A. H. and Wieschaus, E. F. (2005). folded gastrulation, cell shape change and the control of myosin localization. *Development* **132**, 4165-4178.

Dietz, M. L., Bernaciak, T. M., Vendetti, F. and Hildebrand, J. D. (2006). Differential actin-dependent localization modulates the evolutionarily conserved activity of shroom-family proteins. *J. Biol. Chem.* **281**, 20542-20554.

Dollar, G. L., Weber, U., Mlodzik, M. and Sokol, S. Y. (2005). Regulation of Lethal giant larvae by Dishevelled. *Nature* **437**, 1376-1380.

Fairbank, P. D., Lee, C. J., Ellis, A., Hildebrand, J. D., Gross, J. M. and Wallingford, J. B. (2006). Shroom2 (APXL) regulates melanosome biogenesis and localization in the retinal pigment epithelium. *Development* **133**, 4109-4118.

Fristrom, D. (1988). The cellular basis of epithelial morphogenesis. *Tissue Cell* **20**, 645-690.

Gunawardane, R. N., Lizarraga, S. B., Wiese, C., Wilde, A. and Zheng, Y. (2000). gamma-Tubulin complexes and their role in microtubule nucleation. *Curr. Top. Dev. Biol.* **49**, 55-73.

Hacker, U. and Perrimon, N. (1998). DRhoGEF2 encodes a member of the Dbl family of oncogenes and controls cell shape changes during gastrulation in Drosophila. *Genes Dev.* **12**, 274-284.

Hagens, O., Dubos, A., Abidi, F., Barbi, G., Van Zutven, L., Hoeltzenbein, M., Tommerup, N., Moraine, C., Fryns, J. P., Chelly, J. et al. (2005). Disruptions of the novel KIAA1202 gene are associated with X-linked mental retardation. *Hum. Genet.* **118**, 578-590.

Hagens, O., Ballabio, A., Kalscheuer, V., Kraehenbuhl, J. P., Schiaffino, M. V., Smith, P. R., Staub, O., Hildebrand, J. and Wallingford, J. B. (2006). A new standard nomenclature for proteins related to Apx and Shroom. *BMC Cell Biol.* **7**, 18.

Haigo, S. L., Hildebrand, J. D., Harland, R. M. and Wallingford, J. B. (2003). Shroom induces apical constriction and is required for hingepoint formation during neural tube closure. *Curr. Biol.* **13**, 2125-2137.

Hertzler, P. L. and Clark, W. H., Jr (1992). Cleavage and gastrulation in the shrimp Sicyonia ingentis: invagination is accompanied by oriented cell division. *Development* **116**, 127-140.

Hildebrand, J. D. (2005). Shroom regulates epithelial cell shape via the apical positioning of an actomyosin network. *J. Cell Sci.* **118**, 5191-5203.

Hildebrand, J. D. and Soriano, P. (1999). Shroom, a PDZ domain-containing actin-binding protein, is required for neural tube morphogenesis in mice. *Cell* **99**, 485-497.

Holtfreter, J. (1946). Structure, motility and locomotion in isolated embryonic amphibian cells. *J. Morphol.* **79**, 27-62.

Job, D., Valiron, O. and Oakley, B. (2003). Microtubule nucleation. *Curr. Opin. Cell Biol.* **15**, 111-117.

Kam, Z., Minden, J. S., Agard, D. A., Sedat, J. W. and Leptin, M. (1991). Drosophila gastrulation: analysis of cell shape changes in living embryos by three-dimensional fluorescence microscopy. *Development* **112**, 365-370.

Karfunkel, P. (1971). The role of microtubules and microfilaments in neurulation in Xenopus. *Dev. Biol.* **25**, 30-56.

Kominami, T. and Takata, H. (2000). Cellular basis of gastrulation in the sand dollar Scaphechinus mirabilis. *Biol. Bull.* **199**, 287-297.

Lajoie-Mazenc, I., Tollon, Y., Detraves, C., Julian, M., Moisand, A., Gueth-Hallonet, C., Debec, A., Salles-Passador, I., Puget, A., Mazarguil, H. et al. (1994). Recruitment of antigenic gamma-tubulin during mitosis in animal cells: presence of gamma-tubulin in the mitotic spindle. *J. Cell Sci.* **107**, 2825-2837.

Lee, J. Y. and Goldstein, B. (2003). Mechanisms of cell positioning during C. elegans gastrulation. *Development* **130**, 307-320.

Luders, J., Patel, U. K. and Stearns, T. (2006). GCP-WD is a gamma-tubulin targeting factor required for centrosomal and chromatin-mediated microtubule nucleation. *Nat. Cell Biol.* **8**, 137-147.

Meads, T. and Schroer, T. A. (1995). Polarity and nucleation of microtubules in polarized epithelial cells. *Cell Motil. Cytoskeleton* **32**, 273-288.

Messier, P. E. (1978). Microtubules, interkinetic nuclear migration and neurulation. *Experientia* **34**, 289-296.

Müsch, A. (2004). Microtubule organization and function in epithelial cells. *Traffic* **5**, 1-9.

Nance, J. and Priess, J. R. (2002). Cell polarity and gastrulation in C. elegans. *Development* **129**, 387-397.

Nieuwkoop, P. D. and Faber, J. (1994). *Normal Table of Xenopus laevis (Daudin).* New York: Garland.

Nikolaidou, K. K. and Barrett, K. (2004). A Rho GTPase signaling pathway is used reiteratively in epithelial folding and potentially selects the outcome of Rho activation. *Curr. Biol.* **14**, 1822-1826.

Nishii, I. and Ogihara, S. (1999). Actomyosin contraction of the posterior hemisphere is required for inversion of the Volvox embryo. *Development* **126**, 2117-2127.

Perry, M. M. and Waddington, C. H. (1966). The ultrastructure of the Xenopus cement gland. *J. Cell. Sci.* **1**, 193-200.

Picard, J. J. (1976). Ultrastructure of the cement gland of Xenopus laevis. *J. Morphol.* **148**, 193-208.

Prat, A. G., Holtzman, E. J., Brown, D., Cunningham, C. C., Reisin, I. L., Kleyman, T. R., McLaughlin, M., Jackson, G. R., Jr, Lydon, J. and Cantiello, H. F. (1996). Renal epithelial protein (Apx) is an actin cytoskeleton-regulated Na+ channel. *J. Biol. Chem*. **271**, 18045-18053.
Rizzolo, L. J. and Joshi, H. C. (1993). Apical orientation of the microtubule organizing center and associated gamma-tubulin during the polarization of the retinal pigment epithelium in vivo. *Dev. Biol*. **157**, 147-156.
Roberts, S. J., Leaf, D. S., Moore, H. P. and Gerhart, J. C. (1992). The establishment of polarized membrane traffic in Xenopus laevis embryos. *J. Cell Biol*. **118**, 1359-1369.
Rodriguez, O. C., Schaefer, A. W., Mandato, C. A., Forscher, P., Bement, W. M. and Waterman-Storer, C. M. (2003). Conserved microtubule-actin interactions in cell movement and morphogenesis. *Nat. Cell Biol*. **5**, 599-609.
Rogers, S. L., Wiedemann, U., Hacker, U., Turck, C. and Vale, R. D. (2004). Drosophila RhoGEF2 associates with microtubule plus ends in an EB1-dependent manner. *Curr. Biol*. **14**, 1827-1833.
Schoenwolf, G. C. and Franks, M. V. (1984). Quantitative analyses of changes in cell shapes during bending of the avian neural plate. *Dev. Biol*. **105**, 257-272.
Schroeder, T. E. (1970). Neurulation in Xenopus laevis. An analysis and model based upon light and electron microscopy. *J. Embryol. Exp. Morphol*. **23**, 427-462.
Sive, H. L., Grainger, R. M. and Harland, R. M. (2000). *Early Development of Xenopus laevis: A Laboratory Manual*. Cold Spring Harbor, NY: Cold Spring Harbor Press.
Staub, O., Verrey, F., Kleyman, T. R., Benos, D. J., Rossier, B. C. and Kraehenbuhl, J. P. (1992). Primary structure of an apical protein from Xenopus laevis that participates in amiloride-sensitive sodium channel activity. *J. Cell Biol*. **119**, 1497-1506.
Stearns, T., Evans, L. and Kirschner, M. (1991). Gamma-tubulin is a highly conserved component of the centrosome. *Cell* **65**, 825-836.
Sweeton, D., Parks, S., Costa, M. and Wieschaus, E. (1991). Gastrulation in Drosophila: the formation of the ventral furrow and posterior midgut invaginations. *Development* **112**, 775-789.
Viamontes, G. I. and Kirk, D. L. (1977). Cell shape changes and the mechanism of inversion in Volvox. *J. Cell Biol*. **75**, 719-730.
Vize, P. D., Melton, D. A., Hemmati-Brivanlou, A. and Harland, R. M. (1991). Assays for gene function in developing Xenopus embryos. *Methods Cell Biol*. **36**, 367-387.
Yoder, M. and Hildebrand, J. D. (2006). Shroom4 (Kiaa1202) is an actin-associated protein implicated in cytoskeletal organization. *Cell Motil. Cytoskeleton* **64**, 49-63.
Young, P. E., Richman, A. M., Ketchum, A. S. and Kiehart, D. P. (1993). Morphogenesis in Drosophila requires nonmuscle myosin heavy chain function. *Genes Dev*. **7**, 29-41.